Journal of Applied Electrochemistry **33**: 361–366, 2003.

Synergistic effect of 2-mercapto benzimidazole and KI on copper corrosion inhibition in aerated sulfuric acid solution

D-Q. ZHANG*, L-X. GAO and G-D. ZHOU
Electrochemical Research Group, Shanghai University of Electric Power, Shanghai, 200090, P.R. China
*(*author for correspondence, fax: +86 21 65700719, e-mail: zhdq@public9.sta.net.cn)*

Received 19 September 2002; accepted in revised form 10 January 2003

Key words: copper, corrosion inhibition, 2-mercapto benzimidazole, synergistic effect

Abstract

2-Mercapto benzimidazole (MBI) was used as a copper corrosion inhibitor in aerated 0.5 mol L^{-1} H_2SO_4 solutions. The inhibition efficiency (IE) increased with increasing MBI concentration to 74.2% at the 1 mM level. A synergistic effect existed when MBI and iodide ions were used together to prevent copper corrosion in sulfuric acid. It was found that IE reached 95.3% in 0.5 mol L^{-1} H_2SO_4 solutions containing 0.75 mmol L^{-1} MBI and 0.25 mmol L^{-1} KI. X-ray photoelectron spectroscopy (XPS) analysis of the copper samples showed that a (Cu^+MBI) complex film formed on the surface to inhibit the copper corrosion and the iodide ions did not participate in the formation of the inhibitor film. The synergistic effect was attributed to the adsorption of iodide anions on the copper surface, which then facilitated the adsorption of protonated MBI and the formation of an inhibitive film.

1. Introduction

Copper and its alloys are used widely in heating and cooling systems, because of their good thermal conductivity and mechanical properties. Copper is a relatively noble metal, but it can suffer severe corrosion in aerated acidic media. One of the most important methods in the corrosion protection of copper is the use of organic inhibitors. Benzotriazole (BTAH) has been used in industry for several decades as an effective copper inhibitor [1–3]. Its corrosion inhibition has been extensively studied, and depends on temperature, pH and the presence of corrosive ions. For example, BTAH exists predominantly as a protonated species $BTAH_2^+$ at $pH < 1$ [4]. Metal surface usually is positively charged in acidic media [5], and the protonated species would be less strongly adsorbed on the metal surface. This results in reduced inhibition efficiencies of most organic inhibitors in acid solutions. Thus, it is necessary to find new inhibitors against copper corrosion in acidic media.

Synergism has become one of the most important effects in inhibition processes, and it serves as a basis for all modern corrosion inhibitor formulations. The addition of halide ions has been observed to increase the adsorption of organic cations and this can greatly enhance the inhibiting action of an organic compound in acid environments [5]. For example, Wu et al. [6] have shown that a synergistic effect exists when BTAH and KI were used together to prevent the corrosion of copper in aerated sulfuric acid. Schweinsberg et al. [7] also showed that 1-[(1′,2′-dicarboxy)ethyl]-benzotriazole (BTM), a BTAH derivative, had a synergistic effect with KI on the dissolution of copper in aerated sulfuric acid. Controversy exists, however, on the actual role of the iodide ions in relation to the improved organic cation adsorption. Wu et al. proposed that the effect of iodide ions in improving the inhibition efficiency of BTAH worked by improving the adsorption of $BTAH_2^+$ on the copper surface and forming a new Cu (IBTA) complex film through a covalent bond between BTAH and iodide ions [6]. On the other hand, Schweinsberg et al. proposed that the synergistic effect resulted from initial contact adsorption of iodide ions on the copper surface, followed by a decrease in the positive charge on the metal, thereby facilitating the adsorption of protonated BTM [7].

Some other heterocyclic compounds are also effective corrosion inhibitors for copper and its alloys, such as 2-mercaptobenzothiazole (MBT) [8]. It is generally accepted that its inhibition mechanism in neutral and alkaline solution is the formation of an inhibitor film of a (Cu^+MBT) complex on the copper surface, just like the inhibition by BTAH. Because the S atom has strong adsorption for copper, many heterocyclic compounds containing the mercapto group have been developed as copper corrosion inhibitors for different industrial application [9, 10]. We have also investigated a series of heterocyclic compounds containing the mercapto group for copper corrosion inhibition in acidic solution. Thus, 2-mercaptobenzimidazole (MBI) (Figure 1) has the best inhibition effect for copper in aerated acidic

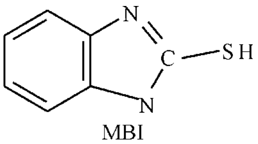

Fig. 1. Structure of 2-mercapto benzimidazole (MBI).

solution [11]. The present work studies the adsorption and inhibitive action of MBI with and without iodide ions for copper dissolution in 0.5 mol L^{-1} aerated H_2SO_4 solution. Corrosion inhibition has been studied by means of polarization curves and electrochemical impedance spectroscopy (EIS). The inhibition efficiencies were determined by coupon tests. X-ray photoelectron spectroscopy (XPS) was used to examine the initial interaction of these compounds with a copper surface.

2. Experimental details

2.1. *Materials*

The working electrode (WE) for the potentiodynamic curves and EIS measurements was prepared from a cylindrical copper rod (99.99%) embedded in polytetrafluoroethylene (PTFE) so that only the circular cross section (0.4 cm^2) of the rod was exposed. The WE was abraded with silicon carbide paper (grade P1200), degreased with AR grade ethanol and acetone, and rinsed with deionized water before use. Coupons for weight loss measurements were circular copper discs (dia. 4.0 cm × 0.15 cm). MBI and KI were AR grade and used as received. All other chemicals were AR grade and the solutions were prepared using deionized water.

2.2. *Apparatus*

Weight loss measurements were carried out by suspending the coupons in 1000 mL vessel placed in a thermostat water bath (40 °C). Electrochemical measurements were performed in a three-electrode cell using a PARC model 283 potentiostat (EG&G) with a PC. A PARC model 1025 frequency response analyser was also used for the EIS measurements. The XPS experiments were performed on a PHI 550 ESCA/SAM spectrometer (Perkin-Elmer). M352 and M398 software packages were used to obtain the polarization curves and electrochemical impedance spectra, respectively.

2.3. *Procedures*

2.3.1. *Weight-loss measurements*

The coupons were abraded with different grades (1, 4 and 6) of emery paper and then washed and degreased with alcohol. They were then dried and rinsed with deionized water. These coupons with freshly prepared surfaces were then fully immersed in the quiescent 0.5 mol L^{-1} H_2SO_4 test solutions containing different levels of inhibitors for four days at 40 °C. Studies were also done in solutions of mixtures of MBI and KI. All solutions were open to air. After the corrosion test, the coupons were rinsed in deionized water and dried. The rinse removed loose segments of the film of the corroded samples. The mean corrosion rates (*CR*) and inhibition efficiencies (*IE*) over the exposure period were then calculated from the following equations:

$$CR = \frac{W_0 - W_1}{A\,T} \tag{1}$$

$$IE = \frac{W_0 - W_1}{W_0} \times 100 \tag{2}$$

where *CR* is in mg cm^{-2} h^{-1}; *A*, the specimen area, is in cm^2; W_0, original weight of the specimen, and W_1, specimen weight after 4 days immersion, are in mg; and *T* the immersion period, is in h.

2.3.2. *Potentiodynamic curve measurements*

The degreased WE were inserted into the solution. After 30 min immersion, the corrosion potential (E_{corr}) was stable. The copper electrode was then polarized with a Pt auxiliary electrode and a saturated calomel electrode (SCE) as the reference electrode. The potential changed from low potential of −900 mV up to +900 mV at speed of 1 mV s^{-1}. All potentials were reported in mV (SCE).

2.3.3. *EIS measurement*

The EIS experiments were performed at open circuit potential over a frequency range of 0.05 Hz to 100 kHz. The sinusoidal potential perturbation was 5 mV in amplitude.

2.3.4. *XPS measurements*

Coupons were mounted on a steel stopper using a molybdenum mask to assure good electrical contact. The analyses were done using a MgK_α X-ray source at 10 kV and 400 W. All analyses were performed at a pressure below 1×10^{-8} torr. The binding energy (BE) values were corrected using the C 1s signal of the atmospheric contaminants (BE = 285.0 eV). The surface films for XPS studies were prepared by immersing the coupons in 0.5 mol L^{-1} H_2SO_4 solutions containing MBI, or mixtures of MBI and KI.

3. Results and discussion

3.1. *Weight-loss measurements*

Corrosion rates of copper coupons were calculated by considering the total affected sample area and immersion times. The average corrosion rates, expressed in mg cm^{-2} h^{-1}, are shown in Table 1. The inhibition of

Table 1. Calculated corrosion rates and inhibition efficiency for weight loss test

Inhibitors	Weight loss /g	Corrosion rates /mg cm^{-2} h^{-1}	*IE* /%
Blank	0.0819	0.0340	–
1 mM MBI	0.0211	0.0088	74.2
0.5 mmol L^{-1} MBI	0.0303	0.0126	63.0
0.1 mmol L^{-1} MBI	0.0682	0.0283	16.7
1 mmol L^{-1} BTAH	0.0342	0.01423	58.2
0.5 mmol L^{-1} BTAH	0.0682	0.02837	16.7
0.1 mmol L^{-1} BTAH	0.0805	0.03349	1.72

BTAH for copper corrosion in the same electrolytes was also done for comparison.

MBI shows increased inhibition with increasing concentration reaching 74.2% at 1 mmol L^{-1} level. BTAH exhibits the same trend with concentration. There are nearly no inhibition effects for BTAH on copper corrosion at the 0.1 mmol L^{-1} level. Thus MBI is seen to be about 20% more efficient as an inhibitor for copper in aerated 0.5 mol L^{-1} H_2SO_4 solution compared with BTAH at a concentration level of 1 mmol L^{-1}. A further series of tests was carried out in 0.5 mol L^{-1} H_2SO_4 containing MBI and KI mixture, which were also compared with a BTAH and KI mixture. The results are shown in Table 2.

The data in Table 2 show that using both MBI and KI in the sulfuric acid solution decreases the corrosion rate more than either BTAH or MBI alone. This indicates that MBI and KI have a synergistic effect to prevent copper corrosion. The corrosion rate of copper is the smallest in the solution containing 0.75 mmol L^{-1} MBI and 0.25 mmol L^{-1} KI, showing that the strongest synergistic effect exists for this condition. MBI has two N atoms in the five-membered ring and one –SH substituent group in the 2-position, and this structure resembles BTAH and MBT. MBI is more likely to form cationic species in acidic solution [12]. It is therefore reasonable to assume that in the present study, the improved corrosion inhibition seen on the addition of KI can be attributed to promotion of the adsorption of MBI cation.

3.2. *Polarization curve measurements*

Figure 2 shows typical polarization curves for copper in aerated 0.5 mol L^{-1} H_2SO_4 with and without KI. The anodic curve for the copper electrode in 0.5 mol L^{-1} H_2SO_4 blank exhibits an initial region of active behaviour and then a limiting current plateau. The current plateau indicates a diffusion-limiting rate, probably the diffusion of copper through the film of $CuSO_4$ formed on the copper surface. The cathodic curves close to the corrosion potential for blank can be ascribed to the reduction of dissolved oxygen present in the test solution. The increase in current density seen at a potential more negative than above −800 mV vs SCE is due to hydrogen evolution. This behaviour is similar to that reported by Tromans [13]. The addition of 1 mmol KI alone to the acid renders E_{corr} more positive. This behaviour was observed by Wu and Schweinsberg [6, 7]. They also reported that in the presence of KI the corrosion rate of copper increased. The cathodic curve in the presence of KI shows a peak (A) at about −580 mV vs SCE and this is most likely due to the reduction of I_2 which spontaneously forms when iodide ions react with dissolved oxygen [14]. In the present study an anodic current peak (B) is also observed on polarization at about −300 mV vs SCE which can be attributed to formation of CuI film on the metal [13]. At a more positive potential the film breaks down leading to an increased metal dissolution rate [13, 15].

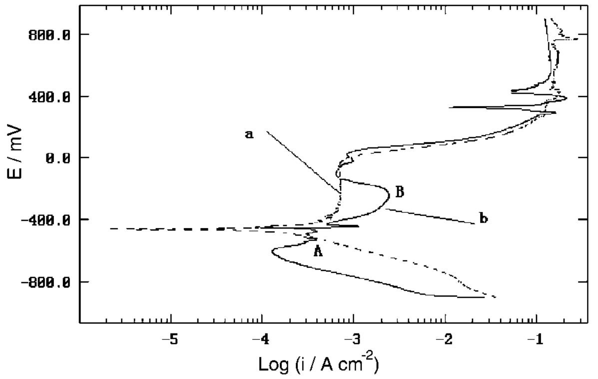

Fig. 2. Polarization behaviour of copper electrode in 0.5 mol L^{-1} H_2SO_4 containing no KI (a) and 1 mmol L^{-1} KI (b).

The polarization behaviour in 0.5 mol L^{-1} H_2SO_4 containing MBI, or MBI + KI mixture is shown in Figure 3. This figure shows that both MBI and the MBI + KI mixture render E_{corr} more negative. With respect to solution containing BTM + KI mixture, the shape of the polarization curve is similar to that observed for KI alone (Figure 2). The presence of a current peak at about −300 mV in the anodic polarization

Table 2. Calculated corrosion rates and inhibition efficiency for weight loss test

Inhibitors	Weight loss /g	CR /mg cm^{-2} h^{-1}	*IE* /%
0.5 mmol L^{-1} BTA + 0.5 mmol L^{-1} KI	0.0265	0.0110	67.6
0.5 mmol L^{-1} MBI + 0.5 mmol L^{-1} KI	0.0051	0.0021	93.8
0.25 mmol L^{-1} MBI + 0.75 mmol L^{-1} KI	0.0113	0.0047	86.2
0.75 mmol L^{-1} MBI + 0.25 mmol L^{-1} KI	0.0039	0.0016	95.3

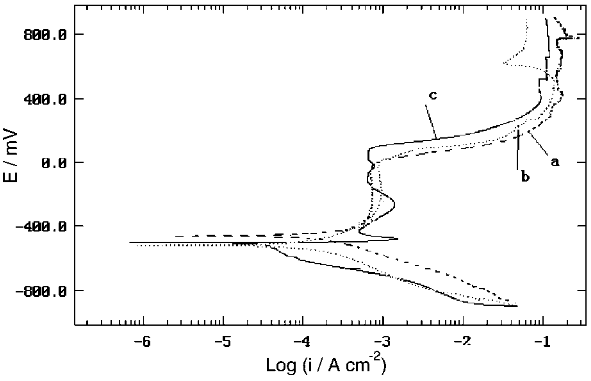

Fig. 3. Polarization behaviour of copper electrode in 0.5 mol L^{-1} H_2SO_4 (a) without and with the addition of (b) 1 mmol L^{-1} MBI and (c) 0.5 mmol L^{-1} MBI + 0.5 mmol L^{-1} KI.

curve can also be attributed to the formation of a CuI film. This is consistent with previous work [6] and shows that BTM and KI do not react with each other to form new phases. The presence of MBI, however, shifted both the anodic and cathodic curves to a lower current density region. The polarization curve of copper in the solution with MBI + KI mixture is very different from MBI alone. It is obvious form Figures 2 and 3, that the cathodic polarization curve of copper in solution containing both MBI and KI is polarized to a greater degree compared to those for copper in the solution having only either MBI or KI. The effect is greater with the mixture of MBI and KI. This result suggests that MBI and KI have a synergistic effect in inhibiting the corrosion of copper in the sulfuric acid.

3.3. *EIS measurements*

The impedance measurements were carried out on copper electrodes in solution containing KI and MBI, as well as their mixture in 0.5 mol L^{-1} H_2SO_4 solutions. Figure 4 shows Nyquist plots for all inhibitors at concentration of 1 mmol L^{-1}. The Nyquist plots exhibit a slightly distorted capacitive semicircle at high frequencies. A higher electrode impedance of the MBI + KI mixture inhibitor was obtained compared with MBI or KI alone. This indicates the inhibition synergistic effect between MBI and KI for copper corrosion in sulfate acid solution.

Impedance spectra of the copper electrode in solutions containing different molar ratios of MBI to KI were also investigated. Figure 5 shows the Bode plots at the total inhibitor concentration level of 1 mmol L^{-1}.

The corrosion resistance of the samples is determined by R_p [16]:

$$R_p = \lim_{\varpi \to 0} R_e\{Z_f\}_{E=E_{\mathrm{corr}}} \qquad (3)$$

where $R_e\{Z_f\}$ represents the real part of the complex faradaic impedance, Z_f, and ω corresponds to the angular velocity of a.c. signal ($\omega = 2\pi f$ where f is frequency (Hz)). R_p corresponds to the horizontal line in a range of low frequencies on the Bode plots. In the case that Bode plots do not show horizontal lines at low frequencies because of limited low frequency range, the impedance modulus value $|Z|$ at the lowest frequency is used to characterize the corrosion resistance [17]. The impedance modulus value $|Z|_{0.05}$ for modulation frequencies f of 0.05 Hz were 3.618 kΩ cm^{-2}, 6.223 kΩ cm^{-2}, 7.158 kΩ cm^{-2} for the copper electrode in a mixture of MBI and KI at the molar ratios of 1:3, 1:1 and 3:1, respectively. These results suggested that the mixture of MBI and KI at molar ratio of 3:1 had the best protection effect, and agreed with earlier results that the larger the $|Z|_{0.05}$ value, the better the corrosion resistance of the electrode [18, 19].

3.4. *XPS measurements*

Figure 6 shows typical XPS survey spectra of the surface of copper samples immersed for 72 h in 0.5 M H_2SO_4 containing MBI solution (MBI/Cu), or MBI + KI solution (MBI + KI)/Cu. An N_{1s} peak at 400.0 eV and an S_{2p} peak at 163.4 eV are present in the spectra of MBI/Cu and (MBI + KI)/Cu, which indicates that

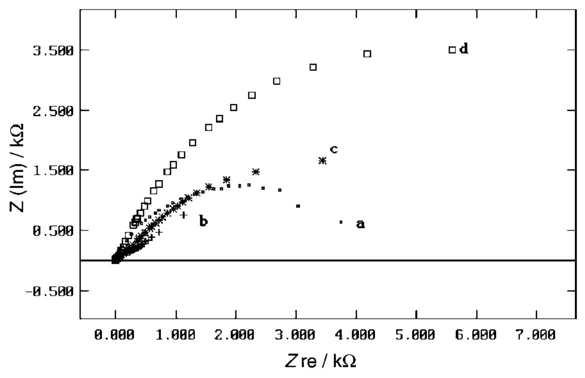

Fig. 4. Nyquist plots of copper electrode in 0.5 mol L^{-1} H_2SO_4 after 2 h immersion without (a) and with 1 mmol L^{-1} KI (b), 1 mmol L^{-1} MBI (c) and 0.5 mmol L^{-1} KI + 0.5 mmol L^{-1} MBI (d).

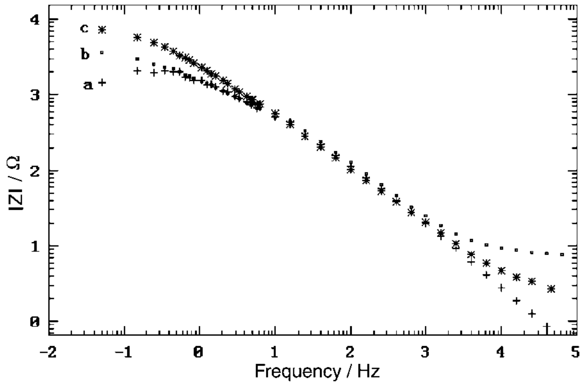

Fig. 5. Bode plots of copper electrode in 0.5 mol L^{-1} H_2SO_4 after 2 h immersion at total 1 mmol L^{-1} mixture inhibitor concentration with different molar ratio of MBI: KI (a) 1:3, (b) 1:1 and (c) 3:1.

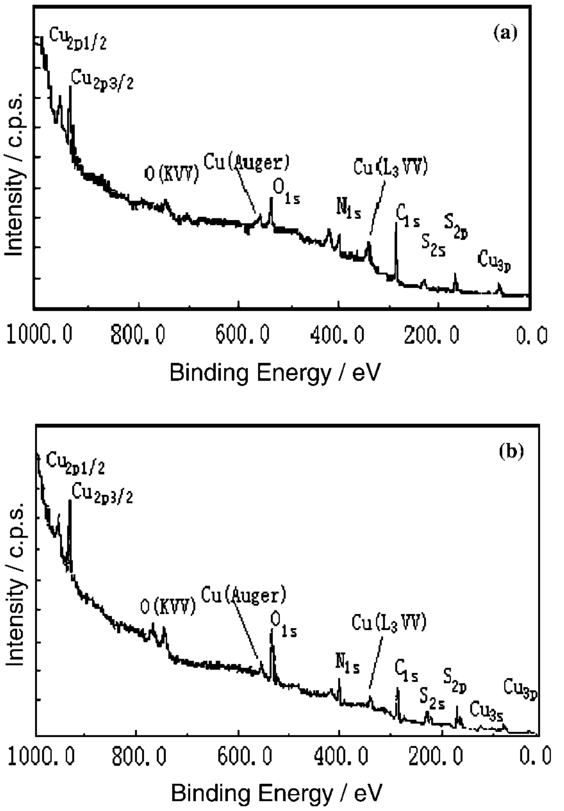

Fig. 6. XPS spectra of copper after immersion in 0.5 mol L^{-1} H_2SO_4 + 1 mmol L^{-1} MBI (a), and 0.5 mol L^{-1} H_2SO_4 + 0.75 mmol L^{-1} MBI + 0.25 mmol L^{-1} KI (b) for 72 h.

MBI film is present on the surface of the copper. A shift of binding energy of N_{1s} and S_{2p} was also been observed compared with those in MBI [8, 9], and this can be explained by the interaction of copper with N and S atoms. The O_{1s} peak may be attributed to oxygen in H_2O, inorganic sulfate, and oxides of copper. The spectrum of (MBI + KI)/Cu does not contain any potassium and iodide peaks (the binding energy of the strongest line is 292 eV for K_{2p} and 620 eV for I_{3d}). This shows that potassium and iodide do not participate in the formation of the surface film on the copper. The composition of the surface can be obtained from the intensity of different elements. The relative amount of the elements is calculated as follows: Cu 5.0%, C 66.3%, N 10.0%, O 8.5%, S 10.1% for the sample immersed in the solution containing only MBI, and Cu 6.4%, C 48.3%, N 11.6%, O 23.9%, S 9.7% for the sample immersed in the solution containing both MBI and KI. The ratio of copper to MBI ($N/2$, the factor 2 is due to the fact that one MBI molecule has two nitrogen atoms) is about 1, indicating that (Cu^+MBI) film forms on the surface when the copper samples are treated in the two cases. It is well known that copper inhibitors such as BTA, MBT can form an inhibitor film consisting of either a (Cu^+BTA) or a (Cu^+MBT) complex on a copper surface [2, 4, 8]. This film can block the dissolution of copper as well as the active site of oxygen reduction.

Figure 7 shows corresponding typical XPS Cu_{2p} spectra. The $Cu_{2p3/2}$ band for copper in the solution containing MBI (MBI/Cu) and the solution containing MBI and KI ((MBI + KI)/Cu) indicates that copper is mainly present in the film in a cation form. It can also be seen from Figure 7 that cupric oxide does not exist on the surface of any of the samples, because a satellite peak around 939.8 eV should be present between the $Cu_{2p3/2}$ peak and $Cu_{2p1/2}$ peak if the film contained cupric oxide. It is generally agreed that cuprous ions is important for forming the (Cu^+BTA) inhibitive film. However, cuprous oxide is thermodynamically unstable in acidic solution [20], so BTAH dose show a high inhibiting effect on copper corrosion in sulfuric acid. It is clear that, the relative amount of the copper atom in the film is larger for the copper sample in MBI + KI solution than that in MBI solution. It is reported that the presence of iodide in sulfuric acid causes the active dissolution behaviour of copper [4]. This effect may be attributed to the formation of the cuprous iodide complex CuI_2^-. The CuI_2^- complex is relatively stable [21], in which the cuprous ions can reaction with protonated MBI to form (Cu^+MBI) film with best corrosion protection. Therefore, the formation of inhibitive (Cu^+MBI) film may be deduced in the following steps:

$$\mathrm{Cu} + \mathrm{I}^- \rightarrow (\mathrm{CuI})_{\mathrm{ads}} + \mathrm{e}^- \tag{3}$$

$$(\mathrm{CuI})_{\mathrm{ads}} + \mathrm{I}^- \rightarrow \mathrm{CuI}_2^- + \mathrm{e}^- \tag{4}$$

$$\mathrm{CuI}_2^- + \text{p-MBI}^+ \rightarrow (\mathrm{CuMBI}) + 2\mathrm{I}^- + p^+ \tag{5}$$

The polarization and surface analytical studies of Wu et al. [6] on the corrosion inhibition of copper in oxigenated solutions of 0.5 mol L^{-1} H_2SO_4 + 0.01 - mol L^{-1} KI + 0.01 mol L^{-1} BTAH led these authors to conclude that inhibition was caused by films composed of $Cu_p(I_mBTA_n)$, where $p = m + n$. SERS investigation by Schweinsberg [7] suggested that enhanced inhibition of iodide ions was first due to adsorption of iodide ions on the copper surface, followed by an overlayer of protonated BTM. Our present work provides evidence

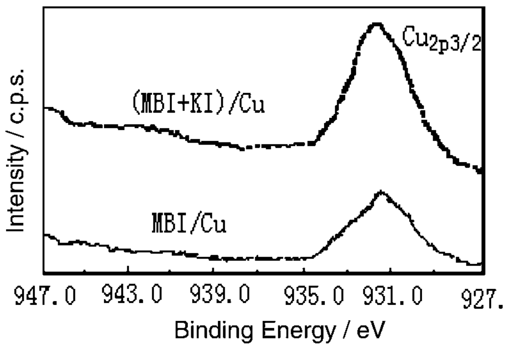

Fig. 7. XPS Cu_{2p} spectra of copper after immersion in 0.5 mol L^{-1} H_2SO_4 + 1 mmol L^{-1} MBI (MBI/Cu), and 0.5 mol L^{-1} H_2SO_4 + 0.75 mmol L^{-1} MBI + 0.25 mmol L^{-1} KI ((MBI + KI)/Cu).

that iodide was not incorporated into the MBI inhibitive film on the copper surface. Its synergistic effect results from initial contact adsorption of iodide anions on the copper, followed by a decrease in the positive in the metal, which improves the adsorption of protonated MBI on the copper surface.

4. Conclusion

The organic molecule, MBI, has a better inhibition effect for copper corrosion compared with BTAH in aerated sulfuric acid solution. The optimum inhibition effect was obtained in 0.5 mol L^{-1} H_2SO_4 solution containing 0.75 mmol L^{-1} MBI and 0.25 mmol L^{-1} KI. XPS results show that the iodide ions do not participate in the formation of the (Cu^+MBI) inhibitor film. The synergistic effect may result from initial contact adsorption of iodide anions on the copper surface, thereby facilitating the adsorption of protonated MBI and the formation of a (Cu^+MBI) inhibitive film.

Acknowledgement

The authors wish to express their appreciation for support from the Key Discipline of Shanghai Education Committee, P.R. China.

References

1. T. Notoya and G.W. Poling, *Corrosion* **326** (1976) 216.
2. F. Mansfeld, T. Smith and P. Parry, *Corrosion* **27** (1971) 289.
3. Y. Ling, Y. Guan and K-N. Han, *Corrosion* **51** (1995) 367.
4. D. Tromans and R. Sun, *J. Electrochem. Soc.* **138** (1991) 3235.
5. I.L. Rozenfeld, 'Corrosion Inhibitors' (McGraw-Hill, New York, 1981), p. 109.
6. Y-C. Wu, P. Zhang, H.W. Pickering and D.L. Allara, *J. Electrochem. Soc.* **140** (1993) 2791.
7. D.P. Schweinsberg, S.E. Bottle and V. Otieno-Alego, *J. Appl. Electrochem.* **27** (1997) 161.
8. M. Ohsawa and W. Suetaka, *Corros. Sci.* **19** (1978) 709.
9. F. Zucchi, G. Trabanelli and C. Monticelli, *Corros. Sci.* **38** (1996) 147.
10. F. Zucchi, M. Fonsati and G. Trabanelli, *Corros. Sci.* **40** (1998) 1927.
11. D-Q. Zhang, L-X. Gao and G-D. Zhou Chin, *J. Appl. Chem.* **19** (2002) 538.
12. G. Lewis, *Corros. Sci.* **22** (1982) 579.
13. D. Tromans and T. Ahmed, *J. Electrochem. Soc.* **145** (1998) 601.
14. C.B. Breslin and W.M. Carroll, *Corros. Sci.* **34** (1993) 327.
15. D. Tromans and J.C. Silva, *J. Electrochem. Soc.* **143** (1996) 458.
16. D.J. Loren and F. Mansfeld, *Corros. Sci.* **21** (1981) 647.
17. G.W. Walter, *Corros. Sci.* **26** (1986) 681.
18. H.H. Ge, G.D. Zhou and Q.Q. Liao, *Appl. Surf. Sci.* **156** (2000) 39.
19. D-Q. Zhang, L-X. Gao and G-D. Zhou, *Acta Phys-Chim. Sin.* **18** (2002) 74.
20. A.D. Modestov, G-D. Zhou and Y-P. Wu, *Corros. Sci.* **36** (1994) 1931.
21. T. Aben and D. Tromans, *J. Electrochem. Soc.* **142** (1998) 398.